Radiocarbon, Vol 60, Nr 5, 2018, p 1413–1424 DOI:10.1017/RDC.2018.94
Selected Papers from the 2nd Radiocarbon in the Environment Conference, Debrecen, Hungary, 3–7 July 2017

RECONSTRUCTION OF SOIL CARBON REDISTRIBUTION PROCESSES ALONG A HILLSLOPE SECTION IN A FORESTED AREA

Tibor József Novák[1*] • Mihály Molnár[2] • Botond Buró[2]

[1]Debrecen University, Faculty of Technology and Sciences, Department of Landscape Protection and Environmental Geography, H-4032, Egyetem tér 1, Debrecen, Hungary.
[2]Isotope Climatology and Environmental Research Centre, Institute for Nuclear Research, Hungarian Academy of Sciences, H-4026, Bem tér 18/c, Debrecen, Hungary.

ABSTRACT. The vertical distribution of soil organic carbon (SOC) with depth and its horizontal pattern is influenced by the topography and relief of the surface, due to lateral redistribution of soil material along slopes. Spatial and temproral variability of these changes is frequently due to human impacts on the landscape. In our study, the results of these processes were studied in detail in a small sub-catchment in a forested hillslope section using radiocarbon (^{14}C) dating of SOC and embedded datable material (charcoal, artifacts) from soil profiles with colluvial accumulations. Events with accelerated material redistribution could be identified as an accumulation of a 40-cm-thick colluvial layer between cal BC 410–360 (2σ) and cal AD 430–580 (2σ). Later colluvial deposition resulted in thinner accumulations (cal AD 1120–1220 [2σ] 30 cm; cal AD 1810–1920 [2σ] 21 cm). As the earliest human impact, we found soil transformation from cal BC 1290–1130 (2σ). The depth-age model for SOC compiled according to the average SOC age and its depth showed different characteristics on middle-slope and down-slope position, with rates of 48.0 yr × cm^{-1} and 22.0 yr × cm^{-1} respectively, which indicates the importance of topographic position of soils in SOC redistribution processes.

KEYWORDS: colluvium, eroded soil, human impact on soil, radiocarbon AMS dating, SOC age, soil landscape.

INTRODUCTION AND AIMS

The radiocarbon (^{14}C) age of soil organic carbon (SOC) pool is subjected to many processes directing the vertical and horizontal pattern of carbon in the soil and exchange between soil and biosphere (Wiaux et al. 2014; Doetterl et al. 2016). Various sources of carbon can modify the ratio of modern and older C in the composition of SOC (Hales et al. 2012). An increasing age of SOC that parallels increasing distance from the soil surface is expected, since most sources of SOC come from litter and biomass production over the soil surface. However, modern C in the form of dissolved organic carbon (DOC) can infiltrate into deeper horizons (Doetterl et al. 2016) in flat areas where infiltration and lessivage is present. This process is less relevant on slopes, where percolation is limited due surface runoff, and in this case it is more likely that soil material redistribution due to lateral translocations will affect the measured age of SOC (Doetterl et al. 2016). Mixing of undecomposed plant remnants by bioturbation, the contribution to SOC of deeply penetrating roots and other subsurface bioproduction (e.g. fungi, bacteria) can also rejuvenate the SOC pool, and shift the measurable ^{14}C age of the soil much younger than the time of soil development (Miao et al. 2016). Where colluvial processes (Zádorová et al. 2015), accelerated erosion (Szalai et al. 2016) or other slope processes not only move the plant remnants and litter, but also SOC-rich soil material moves downslope, the older SOC pool which had earlier accumulated at depth will come closer to the surface. This results in shifting the ^{14}C age to older values than would be expected in a level position. However, where the litter and eroded SOC can accumulate, SOC age will be modified as well. In the case of heavy material movement from deeper soil horizons, older SOC material will be deposited and will increase the age of the SOC pool. If only undecomposed organic material (litter, branches, mulch) are deposited, then at the place of deposition the ^{14}C age will be shifted to be younger ages (Hales et al. 2012). Burial of well-developed, organic-rich soils due to reduced physical exposure and mineralization (Caopricha and Marín-Spiotta 2014; Kirkels et al. 2014) can

*Corresponding author. Email: novak.tibor@science.unideb.hu.

preserve the carbon composition and age signal of its development, which then should indicate the time before burial by younger deposits.

In addition to using direct indication of soil cover transformation (Świtoniak 2014; Świtoniak et al. 2016) and evaluation of remote sensed data (Bertalan et al. 2016), we assume that ^{14}C measurements can contribute in substance to reconstruct the erosion events (Li et al. 2017; Nearing et al. 2017) of a hummocky surface, where slope processes are dominant factors in soil development and organic matter redistribution. However, we note that human influence can have a considerable impact on the soil profile. One of the aims of our study was to determine the extent of this impact. Due to the lack of direct erosion measurements for the area, there was no possibility to estimate erosion rates, which is considerable rather episodic, and not consistent. The aim of this study was to date deposits using ^{14}C data and estimate in an indirect way the volume and time of erosion episodes and their relation to human activities.

STUDY SITE

The study area of Síkfőkút is in the hummocky Bükk-foothill region (Northern Hungary) 47°55′N; 20°26′E, a protected oak (*Quercetum petraeae-cerris*) forest reserve (Szőlőskei-erdő protected area), where there has been no forest management since 1976. At this time the age of the forest was considered to be about 90–100 yr (Stefanovits 1985). According to the general trends of the surrounding area, agricultural land use was previously more extensive and intense (Sütő et al. 2017), but very detailed land use history data are not available for the site. The climate is moderately wet continental with dry summers. The annual mean temperature is 10.0–10.5°C and the average annual precipitation 553 mm (Antal and Justyák 1995). The surface consists predominantly of weathering products of unconsolidated Paleogene marine sediments and Miocene acid volcanoclastic deposits (Gyalog 2005), and the recent surface development is directed by erosional, derasional, and colluvial processes (Dobos 2012). Forest-ecological characteristics of the site have been studied in detail (Antal and Justyák 1995; Varga et al. 2008; Fekete et al. 2017; Tóth et al. 2013), but pedological study of the site has been restricted to generalized characterization of soil conditions (Stefanovits 1985).

METHODS

Three middleslope position (S9; S9/A; S9/B) and three downslope position (S7; S8; S8/B) soil profiles were established along a section (Figure 1) crossing an inactive erosional-derasional valley to identify and localize erosion and accumulation features in soils. Sites with only erosional characteristics could not be included into the sequence, being used as cultivated vineyards, where all of the better-developed (an SOC containing) horizons are completely removed by erosion and the small amount of SOC did not allow ^{14}C dating. Soil profiles were described in the field and classified according the guidelines of the *World Reference Base for Soil Resources* (FAO 2006; IUSS Working Group 2015). From each horizon, soil samples, artifacts, and charcoal pieces, if present, were collected separately. A detailed micro-geomorphological and soil survey was carried out in order to reconstruct the surface development and to estimate their relevance in soil development (Świtoniak et al. 2014; Botos et al. 2015).

Soil samples for general analysis were dried at 40°C for 72 hr and homogenized. Texture was determined according the grain-size distribution, based on analyses made by the sieve and pipette method (Pansu and Gatheyrou 2006). Organic C content was measured by wet oxidation using the bichromate method (Ponomareva and Plotnikova 1980), pH was measured in 1:2.5 H_2O using a standard glass electrode, and inorganic carbonate content was measured by a Scheibler calcimeter (Chaney et al. 1982).

https://doi.org/10.1017/RDC.2018.94 Published online by Cambridge University Press

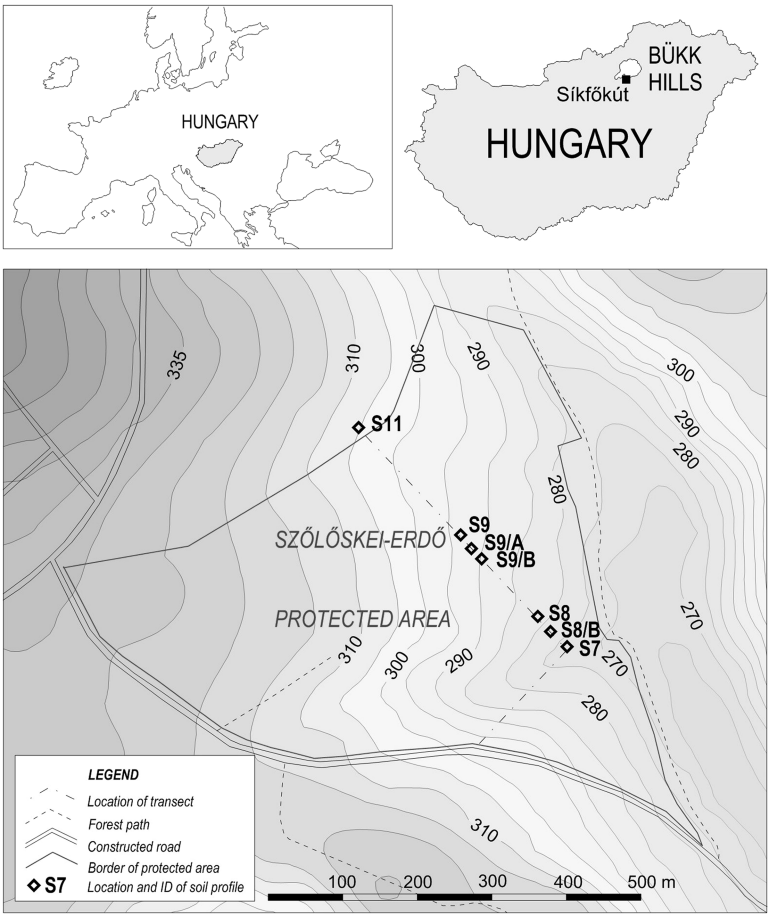

Figure 1 Location of the study site.

Two profiles, one on the midslope (S9/B) with obviously eroded, truncated character but clearly visible human impacts in the form of soil disturbances and a high concentration of charcoal and artifacts, and another one on the downslope (S8/B) consisting of deep colluvial deposits over an older buried soil at a depth of 95–120 cm were chosen for ^{14}C AMS analysis. Charcoal pieces and artifacts collected from both of these and from further profiles (S7, S8) were also included in the evaluation of age data.

For ^{14}C AMS analysis samples from charcoal and brick as well as bulk soil samples were pretreated in the HEKAL AMS laboratory (Molnar et al. 2013a). Inorganic carbonates in soil samples and bricks were removed by 1N HCl at 75°C, for at least 2 hr. Charcoal fragments were separated visually under an optical microscope and treated using the standard acid-base-acid (ABA) method, i.e. in a sequence of 1N HCl, distilled water, 1M NaOH, distilled water, and then 1N HCl HCl at 75°C, for 1–2 hr each step (Molnár et al. 2013a). After the final acid wash, the sample was washed again with distilled water to neutral pH and freeze-dried. For all types of sample materials, a two-step method (charcoal, soil and brick) was applied: first at low temperature combustion (400°C, "LT" fraction) and afterward on the same sample at high temperature combustion (800°C, "HT" fraction) in the presence of high-purity oxygen gas in a

https://doi.org/10.1017/RDC.2018.94 Published online by Cambridge University Press

quartz tube (Jull et al. 2006; Molnar et al. 2013a). The resulting CO_2 gas was then collected and purified separately to form LT- and HT-fractions using an on-line combustion system line and later converted to graphite using the sealed tube Zn-graphitization method (Rinyu et al. 2015).

All ^{14}C measurements were done on the graphitized samples using a compact ^{14}C AMS system (EnvironMICADAS) developed by ETH Zürich (Synal et al. 2007; Wacker et al. 2010), which has been operating at the Hertelendi Laboratory of Environmental Studies since 2011 (Molnár et al. 2013b).

IAEA–C9 (fossil wood) standards were treated and measured in parallel to the samples to check the quality of the preparation. NIST SRM 4990C standard and borehole CO_2 samples were used for normalization of the MICADAS. The results were corrected with the decay of the standard and $\delta^{13}C$ isotopic fractionation. We used the "BATS" software (Wacker et al. 2010) for data reduction of the measured values.

Conventional ^{14}C ages were converted to calendar ages using Calib 7.0.4 software (Stuiver and Reimer 1993) and the IntCal13 calibration curve (Reimer et al. 2013). Calibrated ages are reported as age ranges at the 2-sigma confidence level (95.4%).

The high concentration of C in bulk soil also allowed the ^{14}C dating of SOC and timing of human influence for most profiles. The aim of the ^{14}C dating was to distinguish vertical SOC-age patterns of midslope and downslope (accumulation) profiles and to identify the time of erosion events and human influences.

RESULTS

The upslope profile (S11), located outside of the forest in a cultivated vineyard, was completely eroded without recognizable horizon development (Protic Regosol) and a low amount of soil organic carbon. For the middleslope position soil profiles (S9; S9/A; S9/B), which are exposed to erosion, a repetitive pattern of parallel-tended low ridges was discovered along the slope at 4–5 m distance, dissected by shallow ditches, with 10–40 cm depth. The soil profiles showed therefore high spatial variability related with these surface micro-forms. In most typical positions, Luvisol (S9/B) was identified, which were significantly eroded by the ridges and covered by later colluvic material located in the shallow ditches. The erosion is shown by truncated argic horizons (S9), which were covered in several cases (S9/B; S9/A) by shallow accumulation of colluvial material, showing alteration of erosion and deposition in space and time over a small scale. Downslope profiles were classified as Luvisol (S8), Phaeozem (S8/B), and Umbrisol (S7). The main pedological characteristics of the profiles are summarized in Table 1 and their topographic positions are indicated in Figure 2.

In the case of the middleslope position, anthropogenic influences on the soil profile (S9/B) were observable in the form of layers enriched with artifacts, but the profile and its environment showed truncated horizons, having shallow or missing humus layers at the surface. The horizons at 30–90 cm showed evidence of a strong human influence including dark color, high density of artifacts and charcoal pieces, ceramics, and a disturbed, highly variable soil structure. This horizon was covered by 30-cm-thick colluvial material. The age of bulk SOC of the topsoil at this location is dated to cal AD 950–1020 (2σ) (at a depth of 10–30 cm). ^{14}C ages of bulk SOC samples, charcoals, and artifacts are listed in Table 2.

Accordingly, downslope soil profiles (S8; S8/B; S7) showed accumulation of redistributed colluvial material in thicker layers (Figure 2), in the form of organic-rich colluvic material,

https://doi.org/10.1017/RDC.2018.94 Published online by Cambridge University Press

Table 1 Main characteristics of studied soil profiles.

Profile ID	Elevation (m asl)	Slope (%)	Depth (cm)	Horizon	Texture	Structure	pH (H_2O)	Corg (%wt)	Specific features
S11	304 m	14%	0–25	C1	Silty clay	Strong, coarse, subangular, angular blocky	na.	0.3 ± na.	Cultivated layer
			25–60	C2	Clay	Strong, medium angular blocky	na.	na.	Parent material
S9	297 m	11%	0–11	A	Silty clay loam	Strong, fine subangular, angular blocky	5.2	1.6 ± 0.2	Modern humus layer
			10–60	Bt	Clay loam	Strong, fine to medium angular blocky, prismatic	5.1	0.7 ± na.	Argic horizon
S9/A	295 m	6%	0–45	Ah	Silty clay loam	Moderate, fine-very fine granular, subangular blocky	6.2	3.1 ± 0.4	Modern humus layer
			45–60	Bt	Clay loam	Strong, fine to medium subangular blocky	4.9	0.5 ± na.	Argic horizon
S9/B	293 m	8%	0–10	Ah1	Silty clay	Moderate, fine-very fine subangular blocky	5.5	2.2 ± na	Modern humus layer
			10–30	Ah2	Clay	Strong, fine to medium subangular blocky, platy, prismatic	5.5	1.0 ± 0.2	Colluvial material, artifacts, charcoal
			30–60	Auh	Clay	Strong, fine to medium subangular blocky	5.5	1.1 ± 0.2	High density of artifacts, charcoal
			60–90	2Bt	Clay	Strong, fine angular blocky	6.1	0.7 ± 0.2	Argic horizon
S8	284 m	4%	0–15	Ah1	Silty clay	Weak, fine subangular blocky	5.2	2.4 ± 0.4	Modern humus layer, in colluvial material
			15–45	Ah2	Silty clay	Moderate, fine subangular blocky	5.0	0.9 ± 0.2	Colluvial material
			45–65	Ah3	Silty clay	Strong, fine subangular blocky	5.3	0.8 ± 0.1	Colluvial material
			65–90	2Bt	Clay	Strong, fine angular blocky	5.2	0.7 ± 0.3	Argic horizon
S8/B	284 m	2%	0–15	Ah1	Loam	Strong, fine subangular blocky	5.7	2.4 ± 0.3	Modern humus layer in colluvial material
			15–55	Ah2	Silty clay	Weak, fine granular	5.6	1.4 ± 0.2	Colluvial material
			55–95	Ah3	Loam	Weak, very fine to fine subangular blocky	5.6	1.1 ± 0.1	Colluvial material
			95–120	2Ahb	Clay	Strong, fine angular blocky	5.6	1.5 ± 0.3	Buried soil
			120–140	2Bib	Clay	Strong, fine to medium angular blocky, wedge-shaped	5.6	1.2 ± 0.2	Slickensides, vertic properties
S7	281 m	1%	0–7	Ah1	Loam	Moderate, granular fine to medium	5.2	3.0 ± 0.2	Modern humus layer in colluvial material
			7–20	Ah2	Loam	Moderate, fine to medium granular	5.2	2.3 ± 0.1	Colluvial material
			20–70	Ah3	Clay	Moderate, fine to medium subangular blocky	5.6	1.3 ± 0.1	Colluvial material
			70–100	Ah4	Clay	Moderate, fine to medium subangular blocky	5.3	1.5 ± 0.2	Colluvial material

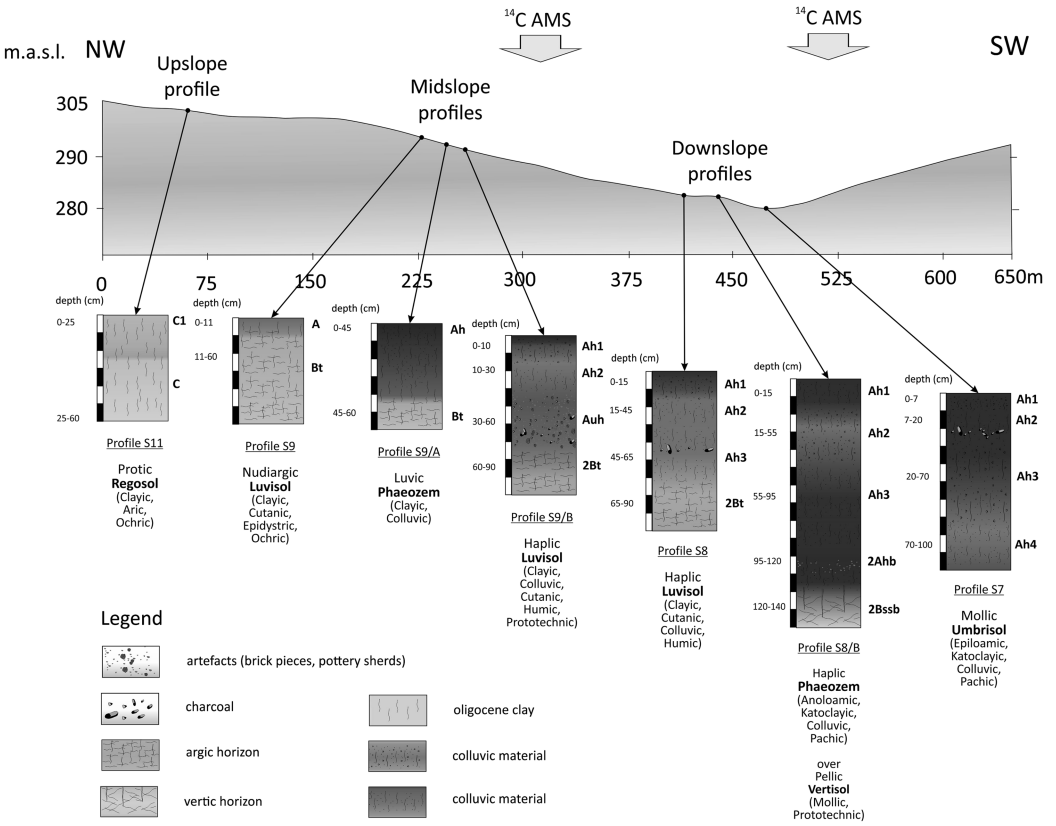

Figure 2 Topographic position and horizonation of studied soil profiles.

occasionally containing artifacts, human-transported materials (such as rock fragments not identical with the basal rocks), and charcoal pieces at different depths. The SOC variability with depth is shown in Figure 3. The thicknesses of colluvial layers vary between 65 cm (S8) and 100 cm (S7) depending on slope steepness and topography. In the case of profile (S8/B), a buried soil layer showing Vertisol characteristics (i.e. slickensides, >30% clay content) could be identified, with higher organic content (1.46 g·kg^{-1}) at a depth of 95–120 cm. It indicates balanced antecedent pedogenesis and in situ carbon sequestration until cal BC 410–360 (2σ), before it was covered by the overlaying younger colluvial material (cal AD 430–580 [2σ]).

DISCUSSION AND CONCLUSION

Reconstruction of Site History

Along the studied slope section we found that upslope soil profiles were completely eroded, midslope profiles showed truncated profile horizonation with shallow colluvic accumulations as a result of alternating erosion and accumulation processes, and colluvic accumulations were found in the downslope position. The thickness of colluvial layers, compared to other sites (Zádorová et al. 2013; Labaz et al. 2018) is rather shallow, which could be related to lower intensity and only periodic relevance of human influences in the study site. The otherwise common aeolian silt mantle (Waroszewski et al. 2018) is missing from the studied profiles, and their clay rich texture does not facilitate erosion and colluvial processes as well. Several events

https://doi.org/10.1017/RDC.2018.94 Published online by Cambridge University Press

Table 2 ^{14}C ages of bulk SOC, charcoal and artifact samples and their pedological characteristics.

Profile ID	Soil reference group	Depth (cm)	Horizon	Material	AMS ^{14}C sample lab code	Conventional ^{14}C age (yr BP)	Calibrated ^{14}C age (2σ)
S9/B	Luvisol	10–30	Ah2	Bulk soil	DeA-12194	1055 ± 25	cal AD 900–920 (0.078) cal AD 950–1020 (0.921)
		30–60	Auh	Bulk soil	DeA-12196	1945 ± 20	cal AD 1–90 (0.937) cal AD 100-120 (0.063)
		55	Auh	Charcoal	DeA-11281	2995 ± 25	cal BC 1370–1360 (0.017) cal BC 1290–1130 (0.982)
		60–90	2Bt	Bulk soil	DeA-12198	3115 ± 30	cal BC 1440–1290 (1)
S8	Luvisol	42	Ah2	Charcoal	DeA-11277	340 ± 20	cal AD 1470–1530 (0.352) cal AD 1540–1640 (0.648)
S8/B	Phaeozem	15–55	Ah2	Bulk soil	DeA-12185	885 ± 25	cal AD 1040–1100 (0.301) cal AD 1120–1220 (0.699)
		55–95	Ah3	Bulk soil	DeA-12187	1540 ± 25	cal AD 430–580 (1)
		95–120	2Ahb	Bulk soil	DeA-11284	2310 ± 25	cal BC 410–360 (0.981) cal BC 270–260 (0.019)
		100–110	2Ahb	Artifact (Brick)	DeA-12192	2335 ± 20	cal BC 410–380 (1)
		120–140	2Bib	Bulk soil	DeA-12189	2690 ± 30	cal BC 900–800 (1)
S7	Umbrisol	21	Ah3	Charcoal	DeA-11279	100 ± 20	cal AD 1690–1730 (0.275) cal AD 1810–1920 (0.725)

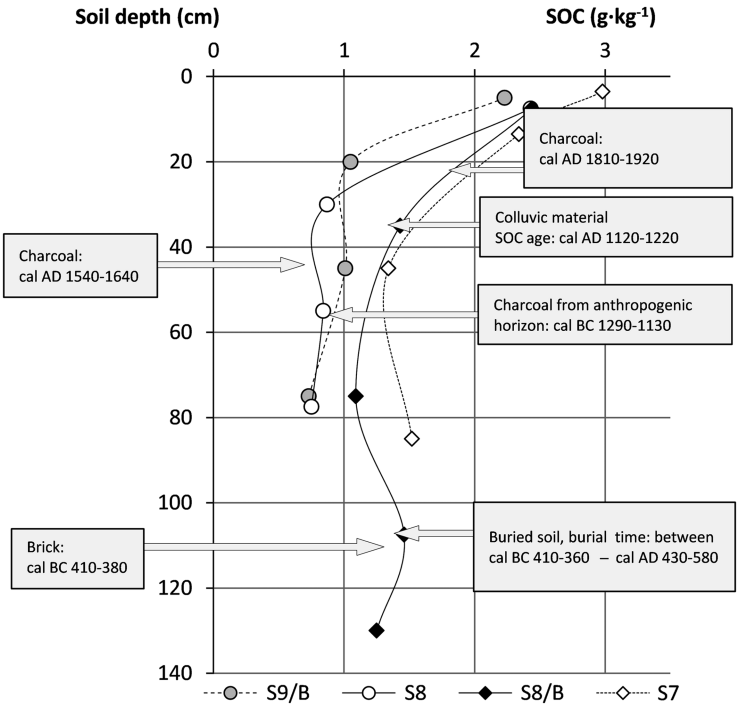

Figure 3 SOC vertical distribution and identifiable events influencing SOC redistribution in studied profiles.

affecting the SOC redistribution and surface development processes could be identified based on ^{14}C AMS data (Figure 3). The earliest human impact can be observed due to the high density of charcoal pieces embedded in anthropogenic disturbed soil layers, mixed with artifacts in profile S9/B, and these date to the late Bronze Age, at cal BC 1290–1130 (2σ). Presumably, the site was inhabited and soil profile rework and truncation can be observed, however, burial and conservation of the old charcoal and artifacts in place is not clearly interpretable, since detailed archeological data are not available, and we do not know if they were buried in situ or transported by colluvial processes. However, later deforestation and the steep slope do not allow for thicker accumulation of younger organic material at location S9, therefore the covering soil even close to the surface has SOC with a conventional ^{14}C age of >1000 ^{14}C yr.

In the valley bottom profile (S8/B), buried artifacts were found at a depth of 110 cm embedded in a buried soil A horizon. Both SOC of bulk buried soil and some brick fragments indicate burial processes from the Iron Age (cal BC 410–360 [2σ], cal BC 410–380 [2σ] respectively). At a depth of 15–55 cm in the same profile (S8/B), the bulk soil SOC indicates an accelerated redistribution of organic rich material from the Medieval era, dated to cal AD 1120–1220 (2σ). This could be related to increasing intensity of land use at that time within the region, similar to other Central and South Europaean sites (Yoo et al. 2006; Dreibrodt et al. 2009; Zádorová et al. 2013).

Charcoal pieces found embedded in colluvial accumulations (S7 and S8) at a depth of 21 and 42 cm depth gave ^{14}C ages of 100 ± 20 BP and 340 ± 20 BP and show that deposition of colluvial material was present even at this time, since the embedding soil SOC has much older age at these depths (885 ± 25 BP and 1055 ± 25 BP, in S9/B and S8/B). Fast deposition of colluvial material

https://doi.org/10.1017/RDC.2018.94 Published online by Cambridge University Press

between the 15th and 20th centuries may be a result of higher anthropogenic activity (e.g. agriculture) in the study area, as it is typical for the land use history in this region (Sütő et al. 2017).

Depending on the rate of carbon sequestration in soil, including gains from primer production and by SOC redistribution by colluvial processes, the rate of burial by overlying material allowed us to calculate a theoretical ratio between SOC age and soil depth for each soil layer (the conventional ^{14}C age of SOC divided by the distance from the surface in cm; Figure 4). This ratio is similar to more sophisticated age-depth models (Simonneau et al. 2013; Gierga et al. 2016), expressing the increase in the apparent age of the SOC with a 1-cm increase in depth. This proved to be different for the middleslope and downslope positions.

Comparing the middleslope S9/B and downslope S8/B profiles, we found that the ages of the carbon pool are increasing with the depth by 48.0 (±6.5) yr · cm^{-1} and 22.0 (±2.2) yr · cm^{-1}, with considerably different rates (Figure 4). According to our expectations, the middleslope profile shows faster aging of soil C with increasing depth than the down-slope profile, as a result of a smaller gain by lateral flux on the middleslope position, and limited accumulation. Presumably, due to alteration by deforestation and revegetation periods caused by land use changes, the changes in C-gain and C-loss were typical during the investigated time. Nevertheless, the higher standard deviation in the erosion profile indicates that SOC redistribution processes have observable variability over time. In any case, the older ^{14}C age of the deeper SOC pool suggests that the different composition of its organic material can have different contributions

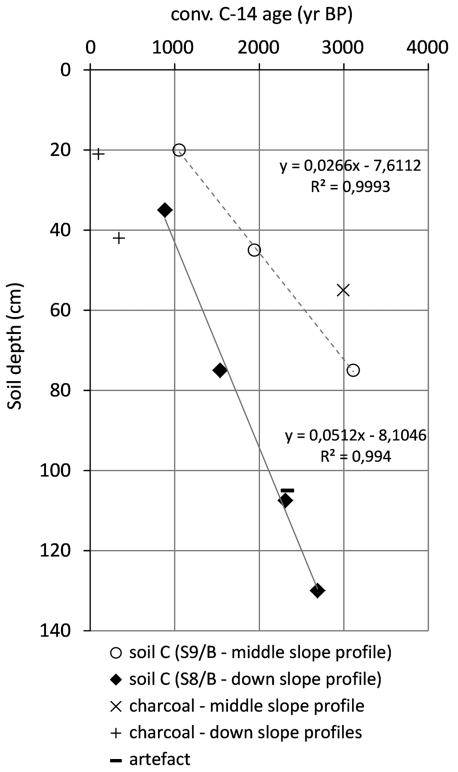

Figure 4 Depth-age model of middle-slope and down-slope soil profiles SOC.

https://doi.org/10.1017/RDC.2018.94 Published online by Cambridge University Press

(Ellerbrock et al. 2016; Premrov et al. 2017) depending on slope position. Bioturbation can also influence the results of SOC-age models, especially if it has different intensity on middleslope and downslope sites. For the study site there is now information about the relevance of this process, but it is supposed to be less intense than in soils with grassland vegetation and having mollic horizons.

The thicknesses of colluvial layers and their historic triggers proved to be similar to those of other Central European sites (Reiß et al. 2009; Dreibrodt et al. 2010, 2013) but this study was useful for reconstructing the SOC accumulation processes related to land use.

SUPPLEMENTARY MATERIALS

To view supplementary material for this article, please visit https://doi.org/10.1017/RDC.2018.94

ACKNOWLEDGMENTS

This research was supported by the European Union and the State of Hungary, co-financed by the European Regional Development Fund in the project of GINOP-2.3.2-15-2016-00009 "ICER".

REFERENCES

Antal E, Justyák J. 1995. Seasonal changes of soil moisture in sessile-oak – Turkey oak forest in Síkfőkút (in Hungarian). In: Tar K, Berki I, Kiss Gy, editors. *Erdő és Klíma (Forest and Climate)*. Debrecen: KLTE. p 106–8.

Bertalan L, Túri Z, Szabó G. 2016. UAS Photogrammetry and Object-based Image Analysis (GEOBIA): erosion monitoring at the Kazár Badland, Hungary. *Acta Geographica Debrecina, Landscape and Environment Series* 10:169–78. http: //doi.org/10.21120/LE/10/3-4/10.

Botos Á, Boda P, Márta L, Novák TJ. 2015. The examination of the cultivation-resulted effects on the soils of Turkey oak forests and sessile-oak forests. *Economica* 8(4/2):225–30. http://real.mtak.hu/31213/1/economica_VIII_2015_4_per_2_szama.pdf.

Caopricha NT, Marín-Spiotta E. 2014. Soil burial contributes to deep soil organic carbon storage. *Soil Biology & Biochemistry* 69:251–64. http://dx.doi.org/10.1016/j.soilbio.201311.011.

Chaney RC, Slonim SM, Slonim SS. 1982. Determination of Calcium carbonate content in soils. In: Chaney RC, Demars KR. 1982. Geotechnical properties, behavior, and performance of calcareous soils. *American Society for Testing and Materials*. Philadelphia-Baltimore. p 3–16.

Dobos A. 2012. Reconstruction of Quaternary landscape development with geomorphological mapping and analysing of sediments at the Cserépfalu Basin (the Bükk Mts, Hungary). *Geomorphologica Slovaca et Bohemica* (1):7–22.

Doetterl S, Berhe AA, Nadeu E, Wang Z, Sommer M, Fiener P. 2016. Erosion, deposition and soil carbon: A review of process-level controls, experimental tools and models to address C cycling in dynamic landscapes. *Earth-Science Reviews* 154:102–22. http://dx.doi.org/10.1016/j.earscirev.201512.005.

Dreibrodt S, Jarecki H, Lubos C, Khamnueva SV, Klamm M, Bork H-R. 2013. Holocene soil formation and soil erosion at a slope beneath the Neolithic earthwork Salzmünde (Saxony-Anhalt, Germany). *Catena* 107:1–14. http://dx.doi.org/10.1016/catena.2013.03.002.

Dreibrodt S, Lubos C, Terhorst C, Damm B, Bork H-R. 2010. Historical soil erosion by water in Germany: scales and archives,chronology, research perspectives. *Quaternary International* 222:80–95. http://dx.doi.org/10.1016/j.quaint.2009.06.014.

Dreibrodt S Nelle O, Lütjen I, Mitusov A, Clausen I, Bork H-R. 2009. Investigations on buried soils and colluvial layers around Bronze Age burial mounds at Bornhöved (Northern Germany) – An approach to test the hypothesis of "landscape openness" by the incidence of colluviation. *The Holocene* 19(3):487–97.

Ellerbrock RH, Gerke HH, Deumlich D. 2016. Soil organic matter composition along a slope in an erosion-affected arable landscape in North East Germany. *Soil and Tillage Research* 156:209–18. https://doi.org/10.1016/j.still.2015.08.014.

Fekete I, Lajtha K, Kotroczó Zs, Várbíró G, Varga Cs, Tóth JA, Demeter I, Veperdi G, Berki I. 2017. Long-term effects of climate change on carbon storage and tree species composition in a dry deciduous forest. *Global Change Biology* 23:(8):3154–68.

Gierga M, Hajdas I, van Raden UJ, Gilli A, Wacker L, Sturm M, Bernasconi SM, Smittenberg RH. 2016. Long-stored soil carbon released by prehistoric land use: Evidence from compound-specific radiocarbon analysis on Soppensee lake sediments. *Quaternary Science Reviews* 144:123–31. http://dx.doi.org/10.1016/j.quascirev.2016.05.011.

Gyalog L, editor. 2005. *Explanations to the Surface Geological Map of Hungary in 1:100 000 Scale*. Budapest: Hungarian Institute of Geology. 189 p. In Hungarian.

Hales TC, Scharer KM, Wooten RM. 2012. Southern Appalachian hillslope erosion rates measured by soil and detrital radiocarbon in hollows. *Geomorphology* 138:121–9. http://dx.doi.org/10.1016/j.geomorph.2011.08.030.

FAO. 2006. *Guidelines for Soil Description*. 4th edition. Rome: FAO. 97 p.

IUSS Working Group WRB. 2015. World Reference Base for Soil Resources 2014 (2015 update). *World Soil Resources Reports* 106. Rome: FAO. 181 p.

Jull AJT, Burr GS, Beck JW, Hodgins GWL, Biddulph DL, Gann J, Hatheway AL, Lange TE, Lifton NA. 2006. Application of accelerator mass spectrometry to environmental and paleoclimate studies at the University of Arizona. *Radioactivity in the Environment* 8:3–23.

Kirkels FMSA, Cammeraat LH, Kuhn NJ. 2014. The fate of soil organic carbon upon erosion, transport and deposition in agricultural landscapes – A review of different concepts. *Geomorphology* 226:94–105. http://dx.doi.org/10.1016/j.geomorph.2014.07.023.

Labaz B, Musztyfaga E, Waroszewski J, Bogacz A, Jezierski P, Kabala C. 2018. Landscape-related transformation and differentiation of Chernozems – Catenary approach in the Silesian Lowland, SW Poland. *Catena* 161:63–76.

Li HC, Burr GS, Löwemark L, Ku TL. 2017. AMS ^{14}C applications. *Quaternary International* 447:1–2. https://doi.org/10.1016/j.quaint.2017.07.033.

Miao X, Wang H, Hanson PR, Mason JA, Liu X. 2016. A new method to constrain soil development using both OSL and radiocarbon dating. *Geoderma* 261:93–100. http://dx.doi.org/10.1016/j.geoderma.2015.07.004.

Molnár M, Janovics R, Major I, Orsovszki J, Gönczi R, Veres M, Leonard AG, Castle SM, Lange TE, Wacker L, Hajdas I, Jull AJT. 2013a. Status report of the new AMS ^{14}C sample preparation lab of the Hertelendy Laboratory of Environmental Studies (Debrecen, Hungary). *Radiocarbon* 55:665–76.

Molnár M, Rinyu L, Veres M, Seiler M, Wacker L, Synal HA. 2013b. ENVIRONMICADAS: a mini ^{14}C AMS with enhanced gas ion source interface in the Hertelendi Laboratory of Environmental Studies (HEKAL), Hungary. *Radiocarbon* 55:338–44.

Nearing MA, Xie Y, Liu B, Ye Y. 2017. Natural and anthropogenic rates of soil erosion. *International Soil and Water Conservation Research* 5:77–84. http://dx.doi.org/10.1016/j.iswcr.2017.04.001.

Pansu M, Gatheyrou J. 2006. *Handbook of Soil Analysis*. Berlin-Heidelberg: Springer Verlag. 35–42.

Ponomareva VV, Plotnikova TA. 1980. *Gumus i Pochvoobrazovanie (Humus and Pedogenesis)*. Leningrad: Nauka. p 65–74.

Premrov A, Cummins T, Byrne KA. 2017. Assessing fixed depth carbon stocks in soils with varying horizon depths and thicknesses, sampled by horizon. *Catena* 150:291–301. http://dx.doi.org/10.1016/j.catena.2016.11.030.

Reimer PJ, Bard E, Bayliss A, Beck JW, Blackwell PG, Bronk Ramsey C, Buck C, Cheng H, Edwards RL, Friedrich M, Grootes PM, Guilderson TP, Haflidason H, Hajdas I, Hatté C, Heaton TJ, Hoffmann DL, Hogg AG, Hughen KA, Kaiser KF, Kromer B, Manning SW, Niu M, Reimer RW, Richards DA, Scott EM, Southon JR, Staff RA, Turney CSM, van der Plicht J. 2013. IntCal13 and Marine13 radiocarbon age calibration curves 0–50,000 years cal BP. *Radiocarbon* 55(4):1869–87.

Reiß S, Dreibrodt S, Lubos CCM, Bork HR. 2009. Land use history and historical soil erosion at Albersdorf (northern Germany) – Ceased agricultural land use after the pre-historical period. *Catena* 77:107–8. http://dx.doi.org/10.1016/j.catena.2008.11.001.

Rinyu L, Orsovszki G, Futó I, Veres M, Molnar M. 2015. Application of zinc sealed tube graphitization on sub-milligram samples using EnvironMICADAS. *Nuclear Instruments and Methods in Physics Research B* 361:406–13.

Simonneau A, Doyen E, Chapron E, Millet L, Vannière B, Di Giovanni C, Bossard N, Tachikawa K, Bard E, Albéric P, Desmet M, Roux G, Lajeunesse P, Berger JF, Arnaud F. 2013. Holocene land-use evolution and associated soil erosion in the French Prealps inferred from Lake Paladru sediments and archaeological evidences. *Journal of Archeological Science* 40:1636–45. http://dx.doi.org/10.1016/j.jas.2012.12.002.

Stefanovits P. 1985. Soil conditions of the forest. In: Jakucs P editor. *1985. Ecology of an oak forest in Hungary. Results of „Síkfőkút Project" 1*. Budapest: Akadémiai Kiadó. p 50–7.

Stuiver M, Reimer PJ. 1993. Extended ^{14}C data base and revised Calib 3.0 ^{14}C age calibration program. *Radiocarbon* 35:215–30.

Sütő L, Dobány Z, Novák T, Incze J, Adorján B, Rózsa P. 2017. Long-term changes of land use/land cover pattern in human transformed micro-regions – case studies from Borsod-Abauj-Zemplén county, North Hungary. *Carpath. J. Earth Environ. Sci* 12(2):473–83.

Świtoniak M. 2014. Use of soil profile truncation to estimate influence of accelerated erosion on soil cover transformation in young morainic landscapes, North-Eastern Poland. *Catena* 116:173–84. https://doi.org/10.1016/j.catena.2013.12.015.

Świtoniak M, Charzyński P, Novák TJ, Zalewska K, Bednarek R. 2014. Forested hilly landscape of Bükkalja Foothill (Hungary). In: Świtoniak M, Charzyński P, editors. 2014. *Soil Sequences Atlas*.

Torun: Nicholaus Copernicus University Press. p 169–81.

Świtoniak M, Mroczek P, Bednarek R. 2016. Luvisols or Cambisols? Micromorphological study of soil truncation in young morainic landscapes – case study: Brdonica and Chełmno Lake Districts (North Poland). *Catena* 137:583–95. http://dx.doi.org/j.catena.2014.09.005.

Synal HA, Stocker M, Suter M. 2007. MICADAS: a new compact radiocarbon AMS system. *Nuclear Instruments and Methods in Physics Research B* 259:7–13.

Szalai Z, Szabó J, Kovács J, Mészáros E, Albert G, Centeri Cs, Szabó B, Madarász B, Zacháry D, Jakab G. 2016. Redistribution of soil organic carbon triggered by erosion at field scale under subhumid climate, Hungary. *Pedosphere* 26(5):652–65. http://dx.doi.org/10.1016/S1002-0160(15)60074-1.

Tóth JA, Nagy PT, Krakomperger Zs, Veres Zs, Kotroczó Zs, Kincses S, Fekete I, Papp M, Mészáros I, Oláh V. 2013. The effects of climate change on element content and soil pH (Síkfőkút DIRT Project, Northern Hungary). In: Kozak J et al., editors. *The Carpathians: Integrating Nature and Society Towards Sustainability, Environmental Science and Engineering*. Berlin Heidelberg: Springer-Verlag. p 77–88.

Varga Cs Fekete I, Kotroczó Zs, Krakomperger Zs, Vincze Gy. 2008. The effect of litter on soil organic matter (SOM) turnover in Síkfőkút site. *Cereal Research Communications* 36:547–0.

Wacker L, Bonani G, Friedrich M, Hajdas I, Kromer B, Němec M, Ruff M, Suter M, Synal HA, Vockenhuber C. 2010. MICADAS: Routine and high-precision radiocarbon dating. *Radiocarbon* 52:252–62.

Waroszewski J, Sprafke T, Kabala C, Musztyfaga E. 2018. Aeolian silt contribution to soils on mountain slopes (Mt. Ślęża, southwest Poland). *Quaternary Research* 89(3):702–17. https://doi.org/10.1017/qua.2017.76.

Wiaux F, Vanclooster M, Cornelis J-T, Van Oost K. 2014. Factors controlling soil organic carbon persistence along an eroding hillslope on the loess belt. *Soil Biology & Biochemistry* 77:187–96. http://dx.doi.org/10.1016/j.soilbio.2014.05.032

Yoo K, Amundson R, Heimsath A, Dietrich W. 2006. Spatial patterns of soil organic carbon on hillslopes: Integrating geomorphic processes and the biological C cycle. *Geoderma* 130(1–2):47–65. doi:10.1016/j.geoderma.2005.01.008.

Zádorová T, Penížek V, Šefrna L, Drábek O, Mihaljevič M, Volf Š, Chuman T. 2013. Identification of Neolithic to Modern erosion–sedimentation phases using geochemical approach in a loess covered sub-catchment of South Moravia, Czech Republic. *Geoderma* 195:56–69.

Zádorová T, Penížek V, Vašát R, Žížala D, Chuman T, Vaněk A. 2015. Colluvial soils as a soil organic carbon pool in different soil regions. *Geoderma* 253–254:122–34. http://dx.doi.org/10.1016/j.geoderma.201504.012.

https://doi.org/10.1017/RDC.2018.94 Published online by Cambridge University Press